

Nanostructured graded-index antireflection layer formation on GaN for enhancing light extraction from light-emitting diodes

R. Dylewicz · A.Z. Khokhar · R. Wasielewski ·
P. Mazur · F. Rahman

Received: 22 August 2011 / Revised version: 23 January 2012 / Published online: 24 April 2012
© Springer-Verlag 2012

Abstract We describe the fabrication and characterization of a randomly etched gallium nitride (GaN) surface for enhancing light extraction from light-emitting diodes. Our technique uses silica spheres as nano-targets in a sputter-etch process and produces a fine-grained surface with features around 35 nm. The textured surface layer acts as a graded refractive index layer with antireflection properties. Measurements show that photoluminescence intensity from such treated surfaces on a GaN LED wafer increases 2.2 times over that from pristine surfaces. These findings are also supported by computer modelling studies described here.

1 Introduction

Light-emitting semiconductor devices often suffer from the mismatch of refractive index between the semiconductor material and the outside medium. The mismatch is usually

large and prevents a large fraction of the light generated within the device from escaping outside. This problem affects most light-emitting diodes (LEDs) because these are made from materials with refractive index in the range of 2.3 to 3.5. The total internal reflection of light then confines most of the generated light to within the LED chip, reducing its apparent brightness and degrading the electrical-to-optical power conversion efficiency. This is a well-known and well-understood problem and various techniques have been devised to enhance the amount of light that comes out of LEDs [1–5]. These include intentionally roughening the LED surface and creating a photonic crystal structure on the emitting facet of the LED. The former is now a commercially established technique and the latter, while technically harder to implement, is also being used but by a limited number of LED manufacturers. Both these techniques effectively open up the escape cone of light striking the semiconductor–air interface and allow more light to spill out of the chip. Whereas photonic crystal structures extract light by a collective diffractive process, random surface roughening at micrometer scale does the same by frustrating total internal reflection of light. Yet another way of enhancing LED brightness is through the use of a refractive index matching layer between LED material and the ambient medium. Layers of zinc oxide and various polymers have been used for this purpose. Here we describe a novel technique for achieving refractive index matching between GaN—a widely used semiconductor for making blue and ultraviolet LEDs—and ambient air. Our technique is based on creating a graded refractive index zone at the top surface of GaN LED wafer material by creating a mesoporous surface. The refractive index within this zone changes gradually from that of GaN to the index of the surrounding medium. The transition reduces total internal reflection, enlarging the escape cone and increasing the amount of light that can be

R. Dylewicz · A.Z. Khokhar · F. Rahman (✉)
School of Engineering, University of Glasgow, Rankine Building,
Oakfield Avenue, Glasgow G12 8LT, UK
e-mail: faiz.rahman@electrospell.com
Fax: +44-141-5793033

Present address:

R. Dylewicz
Lam Research AG, Villach, Austria
e-mail: rafal.dylewicz@lamresearch.com

Present address:

F. Rahman
Electrospell Ltd. Block 7, Kelvin Campus, West of Scotland
Science Park, Glasgow G20 0SP, UK

R. Wasielewski · P. Mazur
Institute of Experimental Physics, University of Wrocław, pl.
Maxa Borna 9, 50-204, Wrocław, Poland

extracted from such material. Our technique relies on creating a nano-textured surface through a non-lithographic dry-etching-based patterning technique. Here we describe our surface nano-roughening process, results of actual photoluminescence measurements from the resulting material, as well as theoretical predictions of graded refractive index layer performance.

2 Nanostructured graded-index layer formation

Making submicron spatial structures gets rapidly more difficult as the size of the structures decreases below 100 nm. High performance optical lithography or electron beam lithography can be used to make very small structures but both make use of expensive tools and are thus not widely available. Since a roughened surface has random surface features, alternative techniques may be possible to create structures at very small length scales.

Different techniques have been reported for fabricating graded-index transition layers on the top of GaN LEDs. Those methods include oblique-angle deposition of ITO nanorod-thin films to form multilayer AR coatings [6, 7]. In the latter, LEDs with GRIN ITO AR coating showed 24.3 % higher light output than LEDs with common dense ITO coating, at an injection current of 20 mA. Another method that was recently demonstrated involved oblique-angle deposition of self-organized Ag island-like nanostructures, followed by dry etching to transfer patterns into *p*-type GaN layer [8, 9]. For the former reference, the nanotextured LED showed 46 % higher light output than a standard LED with unpatterned planar *p*-type GaN, at 100 mA. Improvement in light output power of 30.2 % was achieved for the latter case, for the fabricated antireflective ITO LEDs compared to conventional LEDs, at a bias current of 100 mA. Our non-lithographic pattern formation technique is a more efficient way of achieving this goal. It consists of two distinct steps. First a GaN surface is coated with a submonolayer (typically 10 %) coverage of silica nano-spheres. The coated surface is then treated by a plasma discharge in a reactive ion etching (RIE) machine. These are described in more detail below.

Standard, commercially available GaN blue LED wafers were used in this work. The wafers consisted of a *p*-type 140-nm thick GaN upper layer, a 50-nm thick AlGaIn current blocking layer and 115-nm of active MQW layer (a set of five alternating 3-nm InGaIn wells separated by 20-nm GaN barriers). Underneath these was a highly doped 2.5- μ m thick *n*-GaN layer followed by an undoped GaN layer (4- μ m thick) on a 350- μ m thick double side polished sapphire (Al₂O₃) substrate. A cleaved wafer piece was first coated with a 200-nm thick layer of hydrogen silsesquioxane (HSQ) and then some part of this layer was removed from the centre to form a square cavity. The remaining HSQ

frame all around simply acted as a 200-nm thick spacer. After hard-baking the HSQ spacer, silica spheres, also 200 nm in diameter, were dispensed inside the cavity from a dilute aqueous dispersion. A 2-ml drop was found to be sufficient for this purpose. The silica spheres themselves were produced by a modified Stöber method [10]. The sample was then covered by a clean glass slide coated with an anti-stick coating. Slight pressure was applied to squeeze out excess nano-sphere dispersion from the sides. The entire assembly was then placed in a temperature and humidity controlled environment for 2 hours. After this process the top glass plate was removed and the sample was found to be sparsely coated with a submonolayer coverage of randomly placed silica spheres. Further details of this technique have been published elsewhere [11]. Once the coating process was complete, the sample was placed inside a reactive ion etching tool chamber (Oxford Instruments System 100) and was subjected to a carefully optimized plasma process. An Ar + SiCl₄ gas mixture was used at 1:1 ratio together with RF power of 100 W. The sample was placed on a temperature-controlled platen maintained at 40 °C throughout the process which was carried out for 5 minutes at 40 mTorr background pressure.

3 Microscopic analysis

Once processed, samples were observed with a scanning electron microscope (SEM). As seen in Fig. 1(a), an extremely fine-grained randomly roughened surface was produced. Some GaN pillars were also observed at locations where the silica spheres had originally rested on the surface; the spheres having acted as a mask at these locations. The most probable mechanism for producing such morphological features is that of the sputtering of silica spheres leaving silica fragments on the wafer surface which subsequently acted as randomly placed nano-masks. This has been verified by further examinations that showed that almost all of the silica spheres were consumed in the process (leaving behind their imprints as raised GaN pillars). Moreover, similar experiments done with polystyrene spheres did not show any nano-texturing on the wafer surface as seen in Fig. 1(b) where only GaN pillars created by polystyrene sphere masking are seen. Our technique is thus different from nano-sphere lithography techniques where dry etching is carried out through the interstices of close-packed spheres. That technique produces a regular pattern at significantly larger length scales [12–14]. GaN pillars are a necessary by-product of our process and as seen in the inset to Fig. 1(a), these have a diameter at the top of 180 nm with base diameter of around 257 nm. Thus these pillars that rise up from the surrounding GaN nano-grass background have

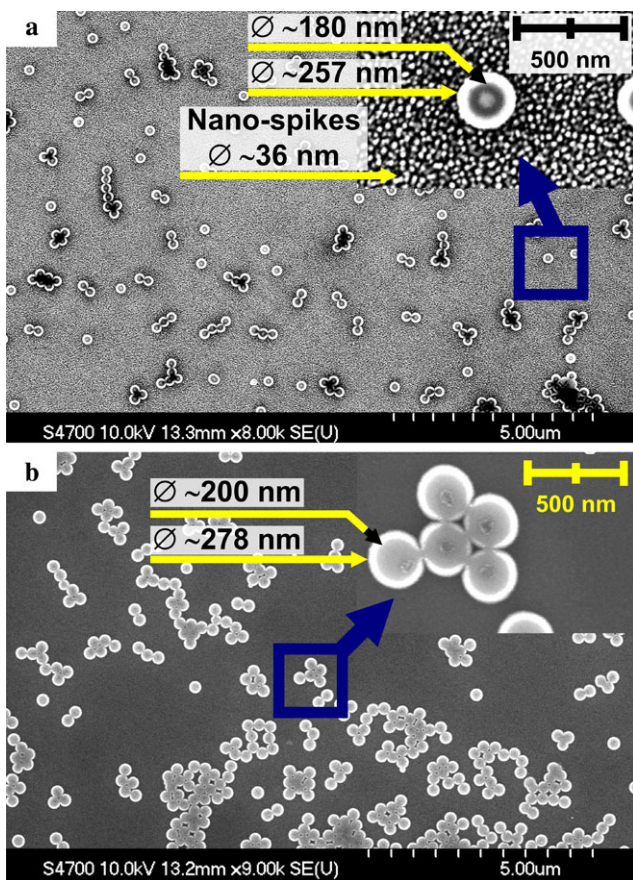


Fig. 1 (a) Scanning electron micrograph of an etched GaN surface showing extremely fine-grained roughness. Also visible are the tops of GaN pillars where silica spheres were originally located. The *inset* shows a close-up view. (b) Similar micrograph of a GaN surface etched with polystyrene spheres. Only a smooth surface was obtained together with GaN pillars

a slope of around 20° . Very similar pillars result from masking with polystyrene spheres but without the production of GaN nano-grass.

The finely etched top *p*-GaN layer of the samples provides a mesoporous surface characterized by conical spaces between GaN spikes. As one moves from the bulk GaN epilayer through this transition layer to ambient air, the refractive index of the medium at ~ 450 nm (emission wavelength for our GaN LED wafer material) gradually changes from 2.4 to 1. The nano-textured GaN surface thus acts as a graded refractive index (GRIN) layer, minimizing the sudden jump of refractive index at GaN–air boundary and thus reducing backreflection of light generated within the GaN/InGaN quantum wells. How the GaN surface nanostructure relates to a graded-index layer is shown in Fig. 2. Figure 2(a) shows an AFM scan of a part of the sample, selected so as to include a couple of nano-pillars as well. A topographic close-up can be seen in part (b) which is color-coded to reveal height differences. These scans were obtained with an ultrahigh vacuum AFM operating in con-

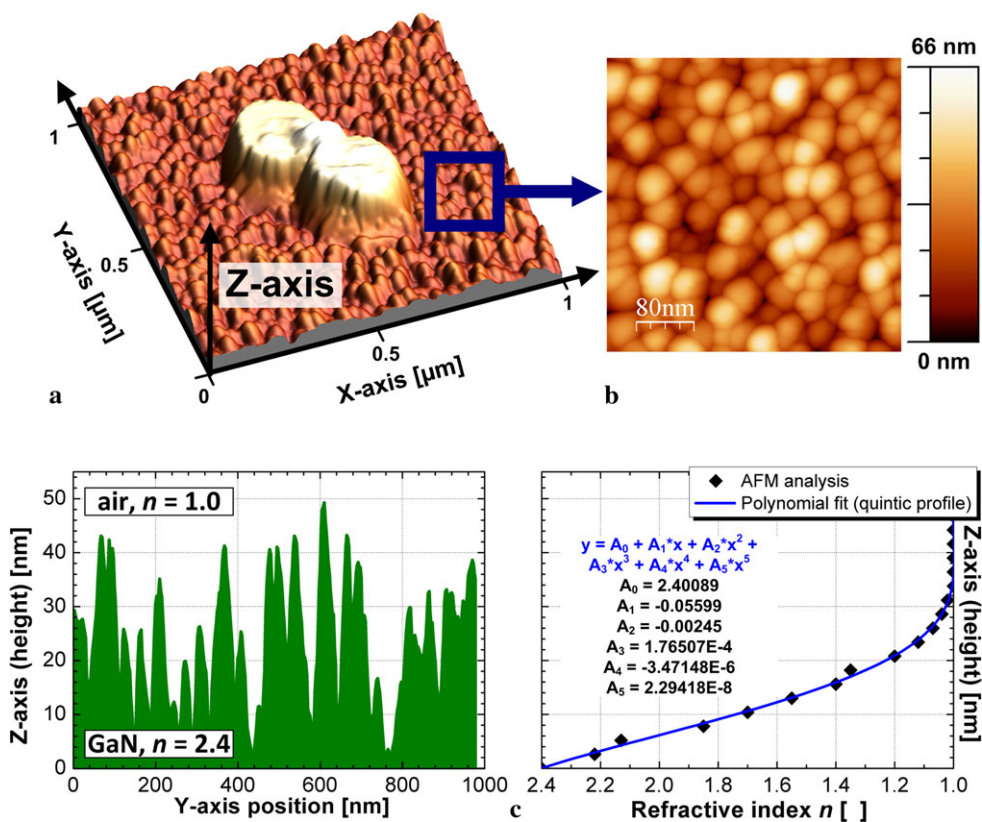
tact mode at room temperature. The scans were additionally processed using WSxM software [15] and revealed random spikes with average height of about 35 nm. From *z*-axis AFM scans the aspect ratio of these structures was measured to be 1:1. Furthermore, the root-mean-square (RMS) roughness of the processed GaN surface was around 9.5 nm, while the same parameter for a smooth, non-etched region was ~ 0.3 nm. This information was used to obtain the average height variation along a typical 1-micron long straight line and the data appears in part (c) (left). Refractive index variation experienced by photons travelling from deep in GaN to the air outside can then be deduced and this variation is depicted to the right in part (c). The refractive index varies linearly at first but after traversing 25 nanometers from the continuous GaN medium the index begins to change very rapidly, approaching unity very quickly from there on. It has been reported that the quintic-index profile shown here is close to the optimum profile for a graded-index antireflection coating [16, 17].

AFM topographic cross section of nano-roughened GaN provided information on the volume fraction of GaN/air along the sample height (Fig. 2(c), left). This, in turn, enabled us to calculate effective refractive index of a composite material, at the given locations within sample height (varied from 0 nm for bulk GaN to ~ 55 nm for pure air). Thus, corresponding data points and the 5th degree polynomial (quintic) fit of refractive-index profile of GRIN GaN layer were finally obtained, as seen in Fig. 2(c) (right).

4 Optical characterization

We performed optical characterization of our samples through angle-resolved photoluminescence (PL) spectroscopy. A sample was illuminated through a 100-mm diameter pinhole by a laser emitting at 405 nm. This has excited PL in the quantum well region of the sample. The emitted light was passed through a long-wavelength-pass filter to block residual pump beam and was coupled to a spectrometer through silica optical fibre that could be rotated around the sample. The spectrometer itself was equipped with a linear silicon array detector. First we measured the normal incidence reflectivity of the sample in the wavelength range of 400 to 1000 nm. This is shown in Fig. 3(a). The % of reflectivity was seen to be lower for a sample with a nanostructured surface with a strong dependence on wavelength. Blue-emitting LEDs will, therefore, benefit more from shallow etched random structures than red-emitting LEDs. Interestingly, for measurements taken in a region where both nano-grass and nano-pillars were present, an even larger reduction in surface reflectivity was observed. It is also possible to examine the influence of surface nanostructuring

Fig. 2 AFM scan showing the morphology of etched GaN surface (a) larger area view of a 1 μm × 1 μm square, showing GaN pillars surrounded by nano-roughened GaN surface. Notice the size contrast between the pillar and the surrounding roughness. (b) A close-up of the same scan. (c) Depiction of the roughness of the GaN surface along an arbitrary line across the sample and the resulting refractive index variation along the z (height) axis



on light travelling from GaN into air. This was done by exciting PL in the sample in the manner described above. Light from PL emission then propagates through GaN and escapes from the top surface. Figure 3(b) shows the angular emission profile (angle-resolved PL) from a nano-textured sample compared with that from an untextured sample. The nano-textured sample shows larger intensities at all angular positions. The integrated intensity was 1.58 times larger for

the nano-textured sample but this value only accounts for the light that is admitted by the optical fibre. The total intensity radiated by the nano-textured sample was even higher (see below). The spectrum of the PL emission from the LED wafer sample can be seen at the top right in Fig. 3(b) where the pump radiation at 405 nm is also seen. We next describe the reason for the increased light extraction observed in our experiments.

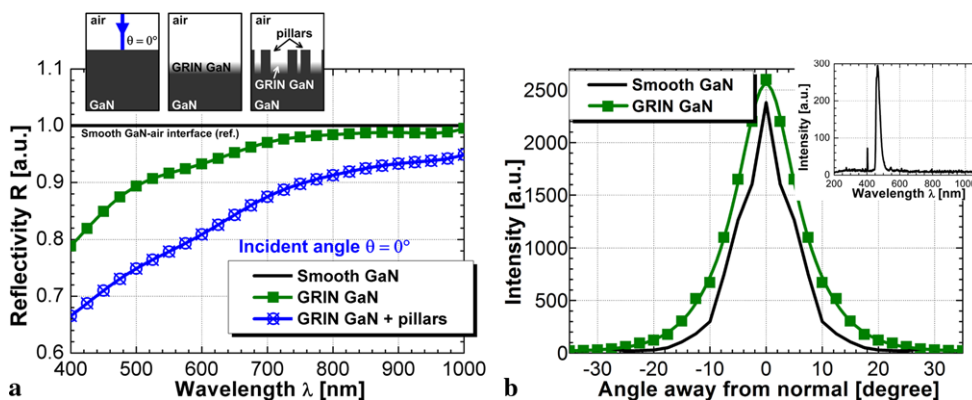
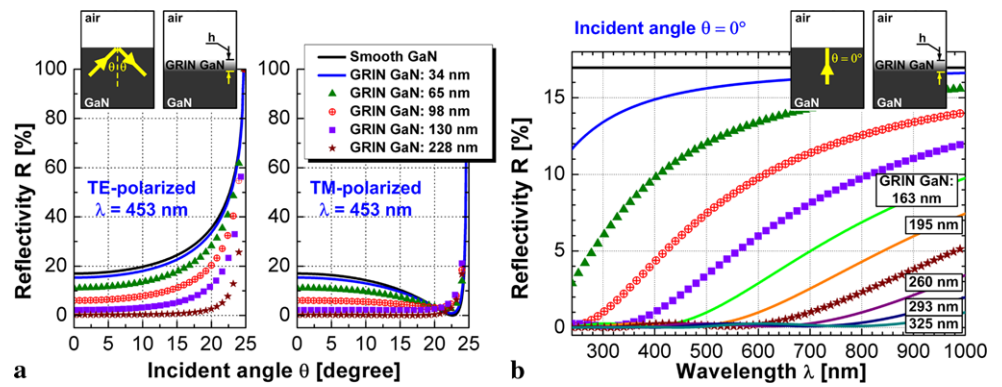


Fig. 3 (a) % of reflectivity as a function of wavelength in the 400 to 1000 nm range for GRIN GaN region (green) and for a region where nano-pillars were also present (blue). (b) Angle-resolved PL from etched (green trace with square points) GaN LED wafer material and

that from non-etched material (continuous black line); both excited by a 405-nm (2-mW) laser beam. The inset depicts a spectrum which shows the PL and the pump laser light

Fig. 4 (a) Predicted % of reflectivity for TE and TM polarizations of 453 nm light incident at GaN–air boundary from the GaN side, as a function of angle of incidence. (b) Predicted % of reflectivity as a function of wavelength for light incident at normal incidence from GaN at the GaN–air boundary. Both plots include cases with different thicknesses of textured GaN material



5 Computer simulations

The optical properties exhibited by such graded structures can be analysed by the Bruggeman effective medium approach [18]. This technique has been utilized in the past to study compositionally-graded dielectric films [19–21] and transparent multilayer stacks [22]. The use of Bruggeman effective medium approximation is preferred over other methods when random pore geometries are encountered. If a regular pore shape is involved then another approximation method such as the Maxwell–Garnett EMA is generally more accurate. The latter was used by Tian et al. [23] in their work on the optical properties of randomly positioned cylindrical pores on silicon surfaces. Their approach was very different from ours as it involved anodic oxidation of thin aluminum films which produces randomly distributed but regularly sized and shaped pores.

In the present case, the Bruggeman equation can be written as

$$V_{\text{GaN}} \frac{n_{\text{GaN}} - n_{\text{eff}}}{n_{\text{GaN}} + (d - 1)n_{\text{eff}}} + V_{\text{air}} \frac{n_{\text{air}} - n_{\text{eff}}}{n_{\text{air}} + (d - 1)n_{\text{eff}}} - 0 \quad (1)$$

with

$$V_{\text{GaN}} + V_{\text{air}} = 1. \quad (2)$$

Here, V_{GaN} and V_{air} are the volume fractions of GaN and air in the nano-textured surface layer, d is a structural dimension parameter which is 1 for our mesoporous layer, while n_{GaN} , n_{air} and n_{eff} are the refractive indices of GaN, air and the effective refractive index of the nano-textured surface. Equation (1) can be iteratively solved using information from AFM scans regarding the relative volume fractions of GaN and air in the textured surface layer. This approach yielded a value of 1.55 for the effective refractive index of the nano-textured layer. Without this layer being present, the critical angle at GaN–air boundary is $\theta_c = 24.6^\circ$, leading to an escape cone angle of 49.2° . With the nano-textured surface interposed between bulk GaN epilayer and air the critical angle for total internal reflection increases to $\theta_c = 40.2^\circ$,

leading to a much wider escape cone angle of 80.4° . For an isotropic light emitter, the former case results in at most 13.7 % of the light managing to come out of the LED chip. In the latter case this is increased to 22.31 %. This would imply that the apparent brightness in the forward hemisphere increases by 1.63 times. However, the increase in brightness measured with an integrating sphere was 2.2—a significantly larger value. We attribute this to the fact that the nano-textured surface is a layer of graded refractive index where the index gradually changes from 2.4 to 1 over a distance of about 35 nm. Such a graded index layer acts as an antireflection layer and is more effective at extracting trapped light than a simple single index layer of glass or zinc oxide as no sudden change in refractive index exists in the case discussed here.

Our GaN nano-grass-based antireflection layer has been modelled by using two-dimensional (2-D) simulations with Cavity Modelling Framework (CAMFR) tool based on the eigenmode expansion method (EEM). CAMFR is a full-vectorial Maxwell solver with an implementation of advanced boundary conditions, i.e. Perfectly Matched Layers (PMLs). EEM leads to a much more compact representation of the field, which drastically improves the simulation accuracy and computing speed, especially when compared with finite difference time-domain (FDTD) methods. The usability of the EEM has been well-proven in the field of photonics to simulate the behaviour of wavelength-scale structures, e.g. photonic crystal devices [24, 25], VCSEL lasers [26], resonant-cavity light-emitting diodes [27] and grating couplers [28, 29]. Additionally, this software is freely distributed under an open source license, i.e. General Public License (GPL) scheme. The nanostructured layer was approximated by using 50 sublayers of equal thickness to constitute a complete graded-index layer. A staircase approximation of a quintic refractive index profile and non-dispersive material properties (complex refractive index independent of wavelength) were used in all simulations. In theoretical calculations of GRIN GaN we assumed that the refractive index of such a layer gradually varies from 2.4 to 1.0 along its thickness, which is based on our experimental AFM observations

presented in Fig. 2. Moreover, for all simulated curves plotted in Fig. 4, a gradual change of refractive index follows the quintic-index profile shown in Fig. 2(c) (right). A polynomial fifth-degree equation was used to fit the experimental AFM data, thus the refractive index value for each of 50 sublayers could be calculated using the equation shown in the inset of Fig. 2(c) (right). Figure 4(a) shows a plot of expected % of reflectivity of GaN–air boundary as a function of angle of incidence (from the GaN side). The reflectivity is seen to drop rapidly as the graded index layer is made thicker with deeper etching. With a layer as deep as 100 nm, a very large fraction of the incident light can easily escape the confines of GaN. The top black line in the plot is for a reference-smooth GaN surface. Part (b) of Fig. 4 shows % of reflectivity as a function of wavelength for normal incidence at the GaN–air boundary. It can be seen that boundary reflectivity is reduced with reduction in emission wavelength and that the presence of a graded-index antireflection layer causes significant further improvement in reflectivity at all wavelengths. The spacing between the various plot lines also indicates that the improvement in reflectivity quickens with increasing depth of etching and the beneficial effects then tend to saturate. This means that such layers can be very effective without being too deep. The advantage of graded-index AR coatings, in contrast to solid thin-film stacks lies in the possibility of providing unlimited antireflection bandwidth together with characteristics independent of incidence angle, as GRIN layers do not critically rely on the precise phase relations typical of interference coatings [30].

Our samples were etched down to only 50 nm (with an average nano-grass peak height of ~ 34 nm) but still clearly show the benefits of a randomly etched mesoporous layer acting as an in situ antireflection component. Even greater benefit can be obtained from an even more deeply etched surface as it can provide a better adiabatic index match between GaN and air; as supported by simulation studies described above. Thus a structurally-integrated mesoporous layer on the emitting face of an LED can be of great use in enhancing its external quantum efficiency. An additional advantage is that the angular emission is featureless without any secondary lobes thus producing uniform brightness suitable for solid-state lighting applications.

6 Conclusions

We have described the fabrication technology for creating nanoscale roughness of the order of a few tens of nanometres on GaN LED wafer material using a non-lithographic technique. Randomly etched features were formed when GaN was locally masked by silica fragments sputtered from

silica spheres purposely deposited on GaN surface with a sparse coverage. The resulting material showed 2.2 times higher extracted PL yield and a featureless angular emission pattern. Simulation studies support the hypothesis that such a layer effectively acts as a graded-index antireflection layer with a quintic profile—reducing the backreflection of light generated inside LEDs. Possible improvements in the patterning process for fabricating nano-porous graded-index GaN layers should lead towards higher aspect-ratio structures. As indicated by theoretical simulations, for average peak height and resulting etch depth in excess of 100 nm, more efficient and broadband AR behaviour can be obtained.

References

1. M.R. Krames, O.B. Shchekin, R. Mueller-Mach, G.O. Mueller, L. Zhou, M.G. Craford, J. Disp. Technol. **3**, 160 (2007)
2. K. McGroddy, A. David, E. Matioli, M. Iza, S. Nakamura, S. DenBaars, J.S. Speck, C. Weisbuch, E.L. Hu, Appl. Phys. Lett. **93**, 103502 (2008)
3. C. Lai, J. Chi, H. Kuo, C. Chao, H. Hsueh, J.T. Wang, W. Yeh, Opt. Express **16**, 7285 (2008)
4. C. Wiesmann, K. Bergenek, N. Linder, U.T. Schwarz, Laser Photonics Rev. **3**, 262 (2009)
5. L. Tian, N. Stojanovic, D.Y. Song, A.A. Bernussi, J.M. Berg, M. Holtz, Appl. Phys. Lett. **91**, 103115 (2007)
6. J.-Q. Xi, M.F. Schubert, J.K. Kim, E.F. Schubert, M. Chen, S.-Y. Lin, W. Liu, J.A. Smart, Nat. Photonics **1**, 176 (2007)
7. J.K. Kim, S. Chhajed, M.F. Schubert, E.F. Schubert, A.J. Fischer, M.H. Crawford, J. Cho, H. Kim, C. Sone, Adv. Mater. **20**, 801 (2008)
8. S. Chhajed, W. Lee, J. Cho, E.F. Schubert, J.K. Kim, Appl. Phys. Lett. **98**, 071102 (2011)
9. Y.M. Song, E.S. Choi, G.C. Park, C.Y. Park, S.J. Jang, Y.T. Lee, Appl. Phys. Lett. **97**, 093110 (2010)
10. W. Stöber, A. Fink, E. Bohn, J. Colloid Interface Sci. **26**, 62 (1968)
11. R. Dylewicz, A.Z. Khokhar, R. Wasielewski, P. Mazur, F. Rahman, Nanotechnology **22**, 055301 (2011)
12. C.B. Soh, B. Wang, S.J. Chua, V.K.X. Lin, R.J.N. Tan, S. Tripathy, Nanotechnology **19**, 405303 (2008)
13. B. Kim, J. Bang, S.H. Kim, J. Kim, J. Electrochem. Soc. **157**, H449 (2010)
14. J.H. Kang, H.G. Kim, H.K. Kim, H.Y. Kim, J.H. Ryu, P. Uthirakumar, N. Han, C.-H. Hong, Jpn. J. Appl. Phys. **48**, 102104 (2009)
15. I. Horcas, R. Fernandez, J.M. Gomez-Rodriguez, J. Colchero, J. Gomez-Herrero, A.M. Baro, Rev. Sci. Instrum. **78**, 013705 (2007)
16. W.H. Southwell, Opt. Lett. **8**, 584 (1983)
17. W.H. Southwell, J. Opt. Soc. Am. A **8**, 549 (1991)
18. M. Khardani, M. Bouaïcha, B. Bessaïs, Phys. Status Solidi C **4**, 1986 (2007)
19. J. Rivory, Thin Solid Films **313–314**, 333 (1998)
20. D.A. Tonova, A.A. Konova, Thin Solid Films **397**, 17 (2001)
21. M. Kildemo, Appl. Opt. **37**, 113 (1998)
22. P. Nubile, Thin Solid Films **342**, 257 (1999)
23. L. Tian, K. Bhargava Ram, I. Ahmad, L. Menon, M. Holtz, J. Appl. Phys. **97**, 026101 (2005)
24. W. Bogaerts, P. Bienstman, D. Taillaert, R. Baets, D. De Zutter, IEEE Photonics Technol. Lett. **13**, 565 (2002)
25. P. Bienstman, R. Baets, Opt. Quantum Electron. **33**, 327 (2001)

26. P. Bienstman et al., *IEEE J. Quantum Electron.* **37**, 1618 (2001)
27. P. Bienstman, R. Baets, *IEEE J. Quantum Electron.* **36**, 669 (2000)
28. D. Taillaert, P. Bienstman, R. Baets, *Opt. Lett.* **29**, 2749 (2004)
29. R. Dylewicz, R.A. Hogg, R. Airey, R. Paszkiewicz, P. Bientsman, S. Patela, *Opt. Quantum Electron.* **42**, 619 (2011)
30. N. Ford, P.W. McMillan, *Glass Technol.* **26**, 104 (1985)